Separation and Purification Technology 285 (2022) 120379

Contents lists available at ScienceDirect

Separation and Purification Technology

journal homepage: www.elsevier.com/locate/seppur

Membrane distillation as a second stage treatment of hydrothermal liquefaction wastewater after ultrafiltration

Ali Sayegh [a], Nikhil Shylaja Prakash [b], Harald Horn [a,b], Florencia Saravia [b,*]

[a] Karlsruhe Institute of Technology, Engler-Bunte-Institut, Water Chemistry and Water Technology, Engler-Bunte-Ring 9, Karlsruhe 76131, Germany
[b] DVGW-Research Center at the Engler-Bunte-Institut, Water Chemistry and Water Technology, Karlsruhe Institute of Technology, Engler-Bunte-Ring 9, Karlsruhe 76131, Germany

ARTICLE INFO

Keywords:
Hydrothermal liquefaction wastewater
Membrane distillation
Optimal flux
Maximum condensate recovery
Wetting mechanisms and analysis

ABSTRACT

The aim of this study is the utilization of membrane distillation (MD) in the treatment of hydrothermal liquefaction wastewater (HTL-WW) to recover ammonium in the condensate. Experiments were carried out using MD under air–gap configuration with HTL-WW pretreated via Ultrafiltration. The results showed membrane stability in long-term operations, up to 36 days and through a wide range of feed temperatures, from 30 °C to 60 °C (Coolant temperature was kept at 20 °C). Feed temperatures, 50 °C and 60 °C provided the best condensate quality, defined by high ammonium concentrations, up to 12 g/L (for 60 °C feed temperature), and low impurity (low contamination by TOC) based on the highest NH_4^+:TOC ratio of 13 (for 50 °C feed temperature). Furthermore, since flux experienced an exponential growth with the increase of feed temperature, 60 °C was chosen as the optimal temperature to expand the study on membrane/condensate recovery, which was performed until 80%. From observational and several analytical methods, wetting was unavoidable above 60% recovery and the cause was credited to organic fouling, mainly via surfactants' adsorption on the membrane surface. This decreased the membrane hydrophobicity, and eventually led to the progressive wetting of the membrane at 80% recovery.

1. Introduction

With population growth and increasing urbanization and industrialization, sewage treatment plants are vital and can have a direct impact on the aquatic ecosystem and also play a central role in ensuring water security in a global scenario of water stress.[1] Relatively high organic load, pathogens in addition to many kinds of toxic substances, such as heavy metals (HMs) and inorganic pollutants are found in the sewage sludge, which is produced in the wastewater treatment plant among separating the liquid and solid parts.[2] However, sewage sludge can also be defined as a potential source of energy and valuable nutrients, which has resulted in a worldwide growth in the energy production via thermochemical processes applied on sewage sludge.[3] For example, hydrothermal liquefaction (HTL), under conditions of high temperature (520–647 K) and moderate pressure (4–22 MPa) can convert wet biomass (5–35% dry solids) into biocrude oil.[4] Due to the release of oxygen and nitrogen contents during the gaseous and aqueous phases of HTL, the biocrude oil product arrives at a similar energy density to that of petroleum.[5]

The produced aqueous phase, also called hydrothermal liquefaction wastewater (HTL-WW), has high concentrations of valuable nutrients and organic carbon which are, respectively, up to 80% and 40% of their content in the feedstock.[6] This relatively high content of organic compounds in HTL-WW, requires development of recovery methods to maintain the economical balance of this process.[7] In addition, discharge of HTL-WW into surface waters is not applicable, because it contains high concentration of ammonia, BOD and other recalcitrant compounds.[8]

One option for treatment of HTL-WW is anaerobic digestion. However, this process can be limited by the high concentrations of ammonia and presence of recalcitrant organic compounds (e.g. phenols) which can be toxic to the anaerobic bacteria.[9] In addition, a microbial electrochemical cell (MEC) is used for the production of hydrogen from HTL-WW, which is affected by the high organic loadings, that can limit the gas production, as well as the wastewater treatment efficiency, especially the removal of recalcitrant compounds.[10]

Recently, wastewater treatment and petroleum industries are adapting membrane technologies as they prove high separation efficiency, low energy consumption and adequate maintenance techniques supported by their relatively stable chemical state.[11] Pressure is one

* Corresponding author.

https://doi.org/10.1016/j.seppur.2021.120379
Received 16 November 2021; Received in revised form 21 December 2021; Accepted 21 December 2021
Available online 24 December 2021

of the driving forces in membrane processes, which are suitable for wastewater treatment. These processes include microfiltration (MF), ultrafiltration (UF), nanofiltration (NF), and reverse osmosis (RO).[12] However, due to the organic and inorganic fouling, periodical cleaning is required for the membrane maintenance and filtration flux regeneration. Such cleaning procedures can mitigate high energy demands and can be expensive.[13]

To minimize the costs, thermally driven processes are recommended, since they can benefit from the residual heat present in the HTL aqueous effluent. For example, membrane distillation (MD) utilizes the heat energy to separate non-volatile nutrients and organic compounds from volatile ones and water.[14] However, membrane wetting represents a major bottleneck for MD and can be accelerated by organic, inorganic and amphiphilic components of wastewater.[15] For example, decrease of surface tension by increasing concentration of organic components leads eventually to the filling of liquid in the membrane pores, hence wetting.[16] Membranes used in MD processes are hydrophobic, which means that the membrane pores have high liquid entry pressure (LEP). However, LEP can be reduced by means of organic fouling consequently leading to the failure of the filtration operation after penetration of the feed liquid into the condensate solution.[17] To minimize the LEP reduction, pretreatment of complex wastewaters via ultrafiltration is recommended, as it can retain particulate and colloidal material, hence improving the permeability, selectivity, and robustness of membrane distillation membranes.[18]

Furthermore, the high cost of commercial ammonia (NH_3) fertilizers rises the agricultural interest in recovery of ammonium nitrogen dissolved in wastewater.[19] As an example, combination of nitrogen gas (from the atmosphere) with hydrogen (from natural gas) via the Haber-Bosch process for the production of NH_3 demands high pressure and temperature in addition to the usage of catalysts,[20] which makes it expensive and contributes to global warming.[21]

The aim of this study is to determine the optimal conditions for treatment, via membrane distillation, of HTL-WW after ultrafiltration pretreatment. Experiments were carried out at several feed temperatures for MD. The main purpose was to find the highest stable flux while concentrating organic carbon in the concentrate and recovering NH_3 in the condensate, taking the quality of the condensate into consideration. In addition, assessment of the maximum achievable condensate recovery is made at the selected temperature. Finally, membrane wetting was analyzed and its mechanisms were discussed.

2. Materials and methods

2.1. Feed solution

The feed solution used in this study is the permeate product from ultrafiltration of the HTL-WW obtained from supercritical, hydrothermal processing of sewage sludge, referred to as HTL-WW_{UF} in this study. More information regarding HTL-WW production and characteristics could be found elsewhere.[22] Ultrafiltration was applied using TiO_2 membrane (Inopor GmbH, Germany) of pore size 10 nm at an average pressure of 1.6 bar and crossflow velocity (CFV) of 0.5 m/s, for removal of suspended solids and oil emulsions.

HTL-WW_{UF} is a turbid black colored liquid, which has a pH value of 9 and electrical conductivity (EC) of 51 mS/cm. The liquid is free of particles, which can be clearly seen in the particle size distribution of the feed stream with 0% recovery in Fig. 4-C representing HTL-WW_{UF}. Elemental analysis was done on carbon, nitrogen, sulfur, phosphorous and other inorganic elements. HTL-WW_{UF} has a total carbon (TC)* concentration of 31 g/L. Total organic carbon (TOC)* represents around 80% of TC and the rest is inorganic carbon mainly in the form of bicarbonate. Volatile fatty acids (VFAs) such as formic, acetic and propionic acid in addition to lactic acid, represent 32% of TOC. Moreover, with lower concentrations, other organic groups such as phenols (0.6 g/L) were detected. Furthermore, larger organic molecules are also present in this liquid such as non-ionic surfactants (1.0 g/L), followed by relatively lower concentrations of cationic (0.2 g/L) and anionic (0.1 g/L) surfactants. Additionally, organic compounds such as stearic acid, palmitic acid and myristic acid were detected in lower concentrations (less than0.1 g/L).

*Although after ultrafiltration TC and TOC shall be equivalent to DC (dissolved carbon) and DOC (dissolved organic carbon), respectively, it was decided to use the terms TC and TOC due to the formation of particulates at high recoveries as shown later in (Fig. 4-C) and discussed in section 3.3.

The cation with the highest concentration is sodium (9.6 g/L), followed by potassium (7.5 g/L). Total Nitrogen presents a concentration of 8.9 g/L, in which 60% is in the form of ammonium and the rest is organic nitrogen. Phosphorous and sulfur (0.5 g/L each) are mainly in the form of phosphate (97%) and sulfate (83%), respectively. Chloride, iron, aluminum and silica are as well quantified and shown in addition to the VFAs in the supplementary material Table 1.

2.2. Membrane distillation setup

Fig. 1 shows the experimental setup of MD. The cell was equipped with a flat sheet membrane unit. The feed channel dimensions are 250 mm × 155 mm × 2 mm and the effective surface area was 0.04 m^2. The experiments were conducted under Air-gap configuration. HTL-WW_{UF} was filled in a feed tank up to a volume of 2.3 L (1 L for experiment no. 6). A magnetic stirrer (VWR International, USA) was used to homogenize the feed solution. Gear pump 1 (ISMATEC, USA) was used to pump HTL-WW_{UF} into the filtration cell Which was then recirculated back into the feed tank. The coolant was pumped via gear pump 2 (ISMATEC, USA) into the cell and was recirculated into the cooling tank. Both gear pumps 1 and 2 were operated at a CFV of 0.05 m/s (volumetric feed flow rate of 0.9 L/min). Thermostats 1 and 2 (Julabo GmbH, Germany), were used to control the temperature in the feed and the coolant. An expanded polytetrafluoroethylene (ePTFE) membrane from W.L. Gore & Associates GmbH (Putzbrunn, Germany) was chosen. The membrane has a pore size of 0.2 µm, thickness of 76 µm and a porosity of 80%. Rhomboidal TENAX CN1 HDPE spacers with a thickness of 2 mm were introduced in the feed and condensate channels. A polypropylene foil separates the coolant from the condensate vapor which condenses on the propylene foil. Flat seals made of fluorinated hydrocarbon were used to support the membrane and the polypropylene foil. The above mentioned details of the filtration cell setup can be found elsewhere.[23] In order to minimize the losses of volatile compounds during recirculation, thermostat 3 (Medingen, Germany) was used as an additional condenser. The condensate was recirculated into the feed tank via a peristaltic pump (ISMATEC, USA), or was collected separately on a balance (Sartorius AG, Germany) using valve V1 for a short period of time for flux measurements. The experiments in this study were performed under the following conditions:

a) Recirculating condition (RC): Here, the valve V1 directs the flow of the condensate back into the feed column after daily sampling and flux calculations were carried out. This configuration was used to run the experiments on a long-term basis to investigate the stability of the flux and to determine the optimum temperature at which the highest possible flux with the best condensate quality could be achieved. In the scope of this work, different filtration conditions were compared based on filtered volume instead of filtration time. The minimum filtered volume representing long-term based experiments was decided to be 100 L/m^2.
b) Concentrating condition (CC): In this case, the valve V1 is closed to condensate recycling and open to continuous collection of the condensate. This configuration aims to concentrate the non-volatile solutes in the feed liquid and provides a deeper understanding on the effect of concentrating of non-volatile solutes on MD.

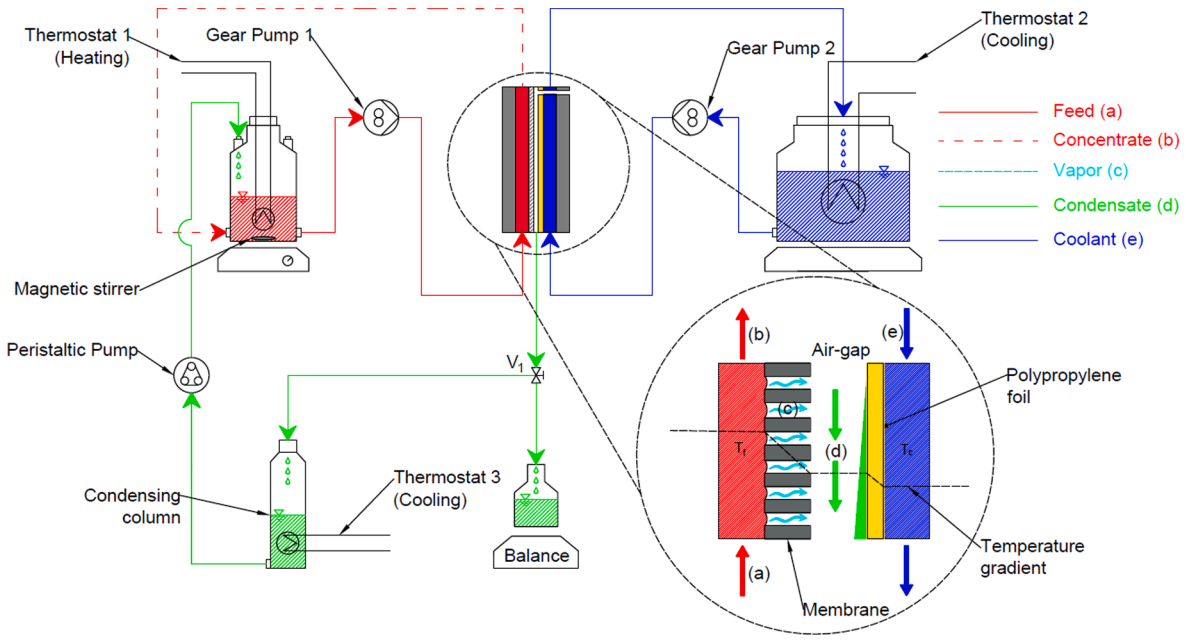

Fig. 1. Experimental setup of air–gap membrane distillation (T_f, and T_c represent feed temperature and condensate/coolant temperature, respectively. T_f varies from 30 °C to 60 °C while T_c is fixed at 20 °C).

c) Integrated conditions: the two conditions RC and CC were used in combination to expand the study. This allowed, at different recovery rates of the condensate, long-term experimental runs of the liquid, and are summarized in Table 1.

A total of 6 experiments were performed using MD. Table 1 provides information on MD experiments. The duration of the experiments ranged from 2 to 36 continuous days. The aim of the experiments 1 to 4 was to evaluate the flux at specific temperatures and to determine the optimal temperature that provides a fast condensate production with the highest quality. Experiments 5 and 6 were performed to evaluate maximum allowable condensate recovery for this wastewater at the chosen temperature and to determine the factors that affect the membrane separation performance at higher recoveries.

Table 1
Overview of conditions of the experiments used for this study (T_f and T_c represent feed temperature and coolant temperature, respectively. RC = Recirculation Condition, CC = Concentration Condition. The arrow → denotes the succeeding condition. The percentage values ×, y and z in RC $^{x\%}$ and CC $^{y\%, z\%}$ represent the stable recovery in RC and the initial and final recoveries in CC conditions, respectively.)

Experiment number	Operation time (h)	Temperature [°C] T_f	T_c	Conditions
1	864	30	20	RC $^{0\%}$ (792 h) ** →CC $^{0\%, 40\%}$ (72 h)
2	288	40	20	RC $^{0\%}$ (264 h) ** →CC $^{0\%, 40\%}$ (24 h)
3	144	50	20	RC $^{0\%}$ (132 h) ** →CC $^{0\%, 40\%}$ (12 h)
4	102	60	20	RC $^{0\%}$ (72 h) ** →CC $^{0\%, 40\%}$ (6 h) → RC $^{40\%}$ (24 h)
5	144	60	20	RC $^{40\%}$ (72 h) → CC $^{40\%, 60\%}$ (6 h) → RC $^{60\%}$ (66 h)
6	48	60	20	CC $^{60\%, 80\%}$ (6 h) → RC $^{80\%}$ (42 h)

** operation time of RC is directly related to the filtered condensate volume of approximately 300 L/m^2

2.3. Analytical methods

Phenols' measurements were performed using test kit LCK 345 from Hach Lange, Germany. Cationic, anionic, and non-ionic surfactants were measured using test kits LCK 331, LCK 332 and LCK 333, respectively from Hach Lange, Germany. Anions (e.g. phosphate, sulfate and chloride), ammonium and organic acids were measured using ion chromatography (IC) (Metrohm, Switzerland). Elements such as sulfur, phosphorous, silica, iron, and aluminum were evaluated using an inductively coupled plasma optical emission spectroscopy (ICP-OES) from Agilent Technologies, USA. Assessment of total carbon (TC), total organic carbon (TOC), total inorganic carbon (TIC) and total nitrogen (TN) concentrations were done using a TOC Analyzer (Shimadzu TOC-V CPN, Japan). Electric conductivity and pH value were measured using a portable multimeter (WTW Multi 350i, Xylem, USA). Particle size distribution (PSD) of HTL-WW$_{UF}$ was measured using Zeta Seizer Nano ZS (Malvern, UK) having a measuring range from 0.6 nm to 6000 nm.

The contact angle (CA) was measured using Contact Angle System OCA (Data Physics Instrument GmbH, Germany). At least 15 measurements were done for every sample and were carried out based on sessile drop technique. The pressure required to cause membrane wetting, also called liquid entry pressure (LEP), was determined using a lab scale cell having a volume of 200 mL (Millipore Amicon, USA). The solution is poured into the cell to the level of 100 mL and homogenized continuously using a magnetic stirrer. Compressed air is used to apply the required pressure with each pressure step having an interval of 24 h. CA and LEP were measured using MD concentrates at different condensate recoveries on the respective fouled ePTFE membranes (Experiments 4 to 6).

2.4. Data interpretation

For this study, the flux, J (LMH) for membrane distillation was calculated as follows,

$$J = \frac{dV}{A\hat{A}\cdot dt} \quad (1)$$

where,dV is the change in volume of the condensate collected (L),dt is interval over which volume is collected (h), andA is the effective

membrane area (m^2).The retention of solutes, R_S (%) by the membrane was calculated using the formula,

$$R_S = \left(1 - \frac{C_c}{C_f}\right) \times 100 \quad (2)$$

where, C_c and C_f are concentrations in condensate and feed in g/L, respectively.

The contamination caused by compound X during membrane distillation to produce ammonium liquid was determined using the following formula,

$$NH_4^+ : X = \frac{C_{NH_4^+,c}/C_{NH_4^+,f}}{C_{X,c}/C_{X,f}} \quad (3)$$

where,$C_{NH_4^+,f}$ and $C_{NH_4^+,c}$ are concentrations of ammonium in feed and condensate in g/L, respectively.$C_{X,f}$ and $C_{X,c}$ are concentrations of compound X in feed and condensate in g/L, respectively.where, X = TOC or phenols

The flux decline ratio (FDR) and flux recovery ratio (FRR) were calculated according to the given Eqs.:[24]

$$FDR(\%) = \left(\frac{J_{PW,NM} - J_{HTL-WW_{UF}}}{J_{PW,NM}}\right) \times 100 \quad (4)$$

$$FRR(\%) = \left(\frac{J_{PW,FM}}{J_{PW,NM}}\right) \times 100 \quad (5)$$

where

$J_{PW,NM}$, $J_{PW,FM}$ are the pure water fluxes of new membrane and fouled membrane (after cleaning with water), respectively, $J_{HTL-WW_{UF}}$ is the HTL-WW_{UF} flux.

3. Results and discussion

3.1. Effect of feed temperature

Throughout experiments 1 to 4, it can be seen that there is an exponential increase in flux, defined in Eq. (1), as a function of feed temperature in case of both pure water (PW) and HTL-WW_{UF} (Fig. 2-A). The flux increased by approximately 3, 6 and 10 times for experiments 2 (40 °C feed), 3 (50 °C feed) and 4 (60 °C feed), compared to experiment 1 (30 °C feed). This exponential increase in flux was in accordance with the Antoine equation for vapor pressure of water shown below:

$$p = \exp\left(23.238 - \frac{3841}{T - 45}\right) \quad (6)$$

where p is the vapor pressure of water in Pa and T is the temperature in K.[25]

As shown in Fig. 2-A, flux in the case of HTL-WW_{UF} was lower than that in the case of pure water for all different feed temperatures. This decrease is relatively stable and can be defined by an average flux decline ratio (FDR) (Eq. (4)) of 15% ± 3%. Non-volatile solutes present in the liquid with high concentrations play a significant role in lowering the vapor pressure by modifying the water activity, hence leading to the Flux decline.[26,27]

As shown in Fig. 2-B, when evaluating the stability of the flux over the filtered volume of 300 L/m^2 and under RC, it was clear that the flux was unaffected and rather stable irrespective of the feed temperature. Furthermore, the flux recovery ratio (FRR), from Eq. (5), after cleaning the membranes with demineralized water were 99% ± 1% for experiments 1 to 4. This is further evidence showing the robustness of the membrane in long term experiments, where the pure water flux is regenerated without the need for any cleaning procedures.

3.2. Optimal flux and condensate quality

Ideally, the highest achievable feed temperature (T_f), which does not affect the membrane material would be the target of any full-scale membrane distillation, as it provides the highest fluxes and hence the fastest production of the condensate. However, presence of volatile and semi-volatile compounds in the feed solution, means that any increase in T_f will lead to increase of transport of these compounds from the feed to the condensate, thus affecting the condensate quality. As a result, the condensate quality is of high importance and only after defining it along with the flux could T_f be chosen. In this study, the target was to produce a condensate which is highly concentrated with ammonium with minimal contamination by other volatiles, measured as TOC.

Based on the temperature and pH value, ammonia in water exists in two forms, volatile ammonia (NH_3) and ammonium ions (NH_4^+).[28] The pK_a of ammonia is 9.25 and as the pH in HTL-WW_{UF} is 9, the fraction of ammonia can range from 40% (at room temperature) to 80% (at 60 °C).[29] Increasing temperature favors production of volatile ammonia in the aqueous solution.[30] This is because rising the temperature leads to lowering the solubility of ammonia, hence resulting in a higher total vapor pressure.[30] Here experiments 1 to 4 are

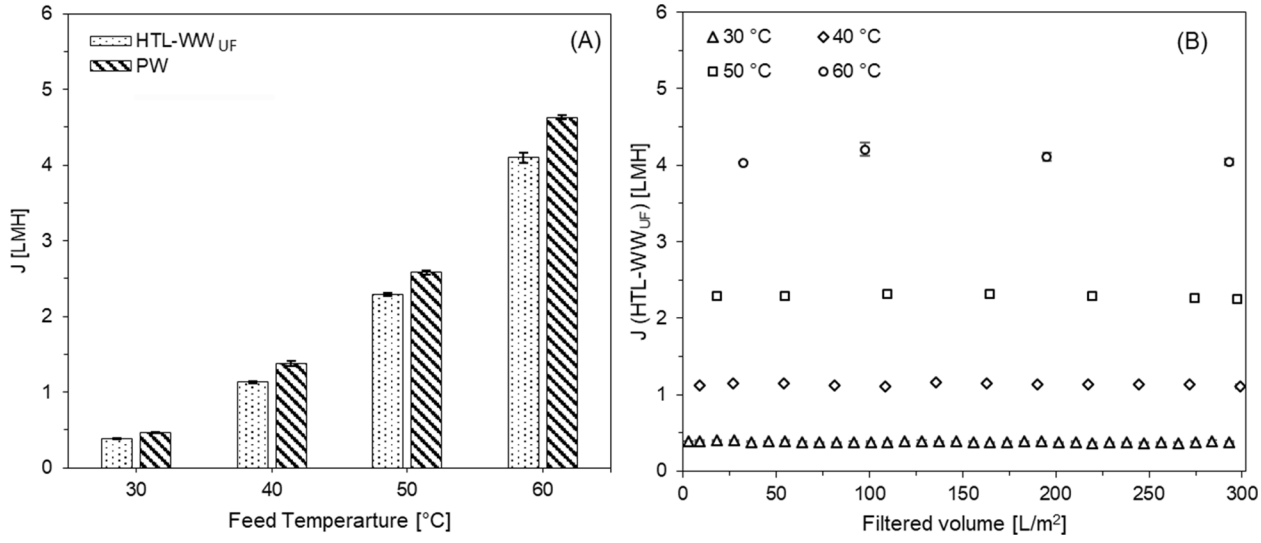

Fig. 2. A) Comparison of flux (J) between $J_{HTL-WW_{UF}}$ for HTL-WW_{UF} and J_{PW} for pure water, and B) Stability of flux $J_{HTL-WW_{UF}}$ under recirculation condition (0 % recovery), for experiments 1 to 4 at different feed temperatures of 30 °C, 40 °C, 50 °C and 60 °C.

compared, until a filtered volume of approximately 60 L/m^2, which is a representation for the total volume of the feed. Fig. 3-A shows increasing ammonium concentration in the condensate with increasing T_f from 6.8 ± 0.5 g/L at 30 °C to 12.4 ± 1.0 g/L at 60 °C, which is almost the double. At a first glance, this gives an idea that higher the T_f is, better is the quality of the condensate produced. However, volatile and semi-volatile organic compounds having higher vapor pressures and boiling points than ammonia can lead to increase in contamination in the condensate at higher T_f. This will increase the TOC concentrations in the condensate with increasing T_f.[31] A significant part (32%) of TOC is VFAs. However, they exist as anions since their pK_a values are in the range of 3.7 – 4.9 and is well below the pH of the liquid, and are hence non-volatile. [32] On the other hand, volatility of other compounds such as p-xylene, benzene, toluene, and MTBE are not influenced by the pH value, but by the vapor pressure, and these compounds can contaminate the condensate at higher feed temperatures (e.g. 50 °C) due to their volatile nature.[33] Hence, it was decided that the quality of the condensate should be analyzed based on the NH_4^+:TOC ratio, defined in Eq. (3). Fig. 3-B presents a pattern that distinctly shows an increase in NH_4^+:TOC ratio until experiment 3 before it slightly decreases for experiment 4. The steady increase of this ratio from experiment 1 (10 ± 1) to 3 (13 ± 1) signifies that the acceleration of ammonium recovery in the condensate is higher than that of volatile organic compounds (VOCs). However, the stability in NH_4^+:TOC ratio until experiment 4 (12 ± 1) suggests that there exists a critical T_f between 50 °C and 60 °C after which the VOCs evaporation accelerates rapidly, hence reducing the quality of the condensate. This critical T_f, is hence recommended for producing the best condensate quality. To further support this, contamination by phenols are examined. NH_4^+:phenols ratio exhibits a similar pattern as seen for NH_4^+:TOC ratio, wherein the maxima were 22 ± 3 and 21 ± 1 at 50 °C and 60 °C, respectively. The relatively high NH_4^+:phenols ratio is due to the high retention of phenols, which was at least 90% for all four experiments. Though the NH_4^+:TOC and NH_4^+:phenols ratios suggest that a critical point between 50 °C and 60 °C is the ideal T_f, the flux at 60 °C feed (4.1 LMH) is significantly higher than that at 50 °C (2.3 LMH) and also the contamination by TOC is not significantly higher than 50 °C. For this reason, 60 °C was chosen as the optimal T_f for further evaluation experiments 5 and 6.

3.3. Maximum achievable condensate recovery

Data from experiment 4 to 6 were used to evaluate the stability of flux at different condensate recoveries. As shown in Fig. 4-A the normalized flux decreased slowly from 0% recovery until 40% recovery, where it reached 95% ± 1%. The first significant decline down to 89% ± 2% was observed at 50% recovery, followed by 81% ± 3% at 70% recovery. This decrease in the flux can be attributed to the increasing feed concentration and the reduction of the following: water activity, mass transfer coefficient, caused by concentration polarization, as well as the heat transfer coefficient, caused by decline in membrane surface temperature.[34] In addition, fouling can lead to the flux decline and can be summarized in three types, 1) Biofouling 2) inorganic fouling (scaling) and 3) organic fouling.[35] It is very unlikely to examine biofouling because bacterial growth is limited by the high ammonia concentration and the presence of recalcitrant organic compounds (e.g. phenols). Also, absence of significant concentrations of magnesium and calcium means that scaling effect is negligible.

However, organic fouling is most likely to be observed for several reasons. First, the initial organic carbon concentration of 24 ± 1 g/L is already high, and gets even higher with the increase in condensate recovery, until reaching 95 ± 2 g/ L at the 80% recovery, which is four times the initial value. This raises the possibility of adsorption of organic compounds on the hydrophobic membrane surface, especially surfactants which have lipophilic characters. Second, even after the ultrafiltration pretreatment, it is known that presence of coagulants (iron, aluminum and silica) can cause agglomeration of organic compounds leading to the formation of colloids and particles. In addition, when the surfactants concentrations exceed the critical micelle concentration, micelles are formed. Entrapment of colloids or particles at the membrane-liquid interface by interfacial tension forces can lead to particulate fouling.[34] At this stage, suspended solids can accumulate on the membrane surface and inside the membrane pores, forming a cake layer which puts on extra thermal and hydraulic resistance to the process. This leads eventually to decreasing the temperature difference across the membrane, and hence a reduction in the driving force.[36] Formation of colloids and particulates was examined using the particle size distribution (PSD) at the different condensate recoveries (Fig. 4-C). With a single peak at 0.7 nm, filtration with 0% recovery (at RC) starts with the absence of particulates. At 40% recovery, the main peak appears at 6 nm, which reveals the formation of small colloids. At 60% recovery, dissolved substances agglomerate and bigger colloids and even particles are formed, which can be clearly seen with the appearance of peaks in the particulate region (>450 nm). As a result, it can be assumed that particulate fouling/cake formation starts between 40% and 60% recovery, and its effect increases with increasing recovery. Until 70% recovery, the fluxes were relatively stable at each recovery. However, at 80% recovery, the normalized flux was stable only for the first 24 h at 73% ± 1%, but rapidly increased to 93% ± 4% after 48 h

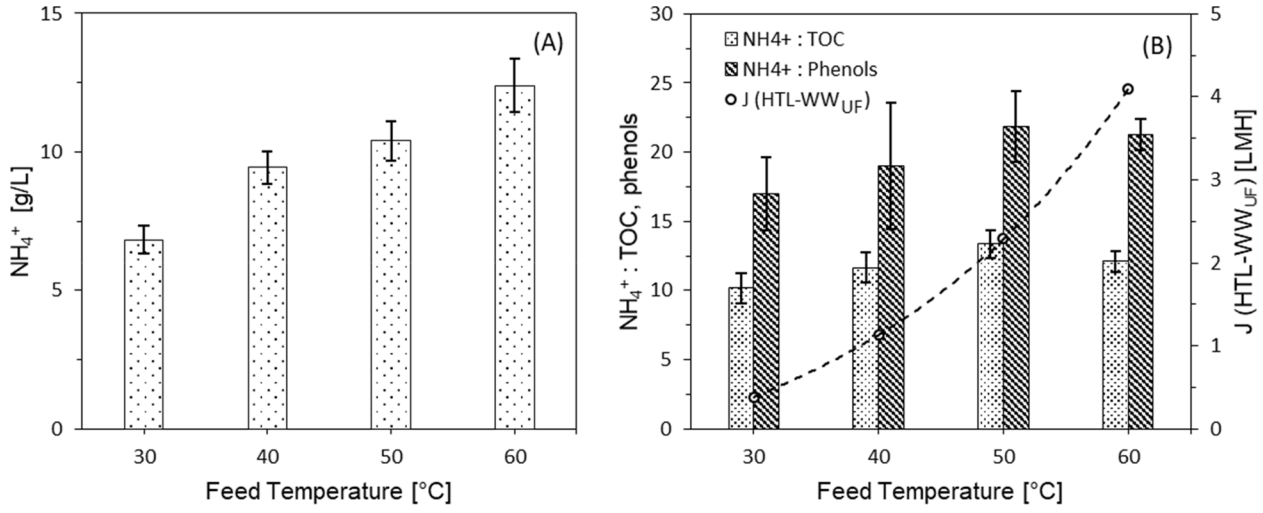

Fig. 3. A) NH_4^+ in condensate and B) Comparison between NH_4^+:TOC, NH_4^+:phenols ratio and flux $J_{HTL-WW_{UF}}$ for experiments 1 to 4 at different feed temperatures of 30 °C, 40 °C, 50 °C and 60 °C.

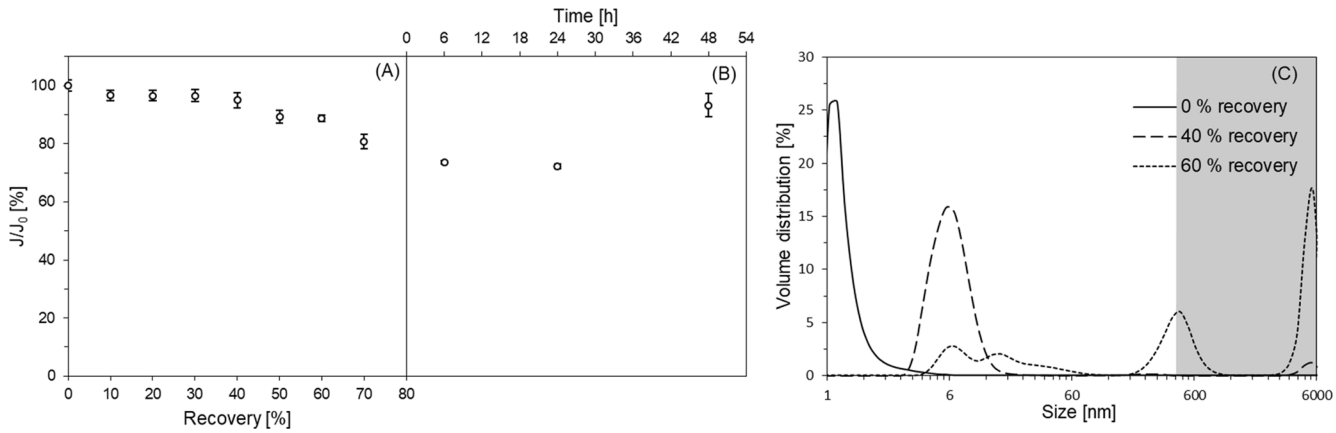

Fig. 4. Normalized flux (J/J_0) at A) different condensate recoveries and B) time dependent development for 80% recovery and C) Particle size distribution (PSD) of feed streams with different recoveries (0% recovery is representable for initial HTL-WWUF feed solution; the grey area (>450 nm) shows the zone with suspended particles).

(Fig. 4-B). Analysis on the membrane and condensate composition showed wetting, which is analyzed in the next section 3.4.

3.4. Wetting analysis

In order to understand the limit of membrane distillation for treatment of HTL-WW_{UF}, it was necessary to observe the exact recovery at which wetting occurred. Initially, simple visual observation of the condensate color and turbidity was done. Until 50% recovery, the color is transparent (Fig. 5-A). A light-yellow color starts to appear at 60% recovery and is more pronounced at 70% recovery. At 80% recovery, the color becomes brown, turbidity increases, and it aggravates over time and eventually at 48 h, the color almost resembles the HTL-WW_{UF} (Fig. 5-B). However, since characterization of HTL-WW_{UF} is incomplete (e.g., less than 50% of TOC is quantified), color indication can't be a concrete method in determining the exact wetting point.

In automated systems, continuous measurement of the electrical conductivity (EC) is applied to detect wetting. This method can as well be used in this work, but with some limitations. Due to the presence of volatile and semi-volatile compounds in the feed solution especially ammonia, some of these compounds are supposed to accumulate in the condensate, leading to a relatively high EC in the condensate. It is however less than the feed EC and stabilizes with time as ammonia gets exhausted as seen in Fig. 6-A. This Fig. clearly depicts that throughout experiment 5 (until filtered volume of 556 L/m^2), EC was decreasing, meaning that no wetting could be seen for both 40 and 60% recoveries. Yet, from the beginning of experiment 6, EC sees a sudden rise, which is at 70% recovery. This proves that the break through point of wetting happens at 70% recovery. EC increases then rapidly to more than 31 mS/cm when reaching 80% recovery at 820 L/m^2 after 48 h, hence implying complete wetting.

Detailed analytical measurements were further applied to support the earlier conclusion. As shown in Fig. 6-B, retention (Eq. (2)) of non-volatile solutes until 60% recovery was greater than 99%. At 70% recovery, slight leakage of these solutes starts with silica, whose retention is only 93%, hence the beginning of wetting. At 80% recovery, more solutes start leaching to the condensate side until the complete wetting happens after 48 h where some solutes retentions went down to around 70%.

Wetting analysis was done on the change of the membrane characteristics after experiments 4, 5 and 6. Contact angles (CA) of the concentrate solutions were measure for the corresponding used membranes. Initially, contact angle of pure (Milli-Q) water on a pristine ePTFE membrane is 138°. Maintaining a contact angle value higher than 90° is essential for preserving the hydrophobic character of the membrane and preventing wetting. The lower the polarity of the droplet (such as for HTL-WW_{UF}), the more it flattens with the membrane surface and hence decreases the CA. Even during filtration, organic fouling plays a major role in modifying the membrane surface characteristics towards less hydrophobic. As shown in Fig. 6-C, CA exhibits a decrease with increasing condensate recovery. After experiment 4, it can be assured that no wetting could have happened at 40% recovery where the CA is far from the wetting limit. For experiment 5, however, it can be said that the membrane is very close to lose its hydrophobicity at a recovery of 60%, as the CA almost reaches the wetting limit. On the other hand, CA for experiment 6 is clearly lower than the hydrophobic limit, hence wetting could be clearly expected when reaching 80% recovery.

Similar to CA, liquid entry pressure (LEP) of the earlier mentioned membranes is in line with the observation of wetting. As seen in Fig. 6-D, LEP decreased by 17% and 87% for experiments 5 and 6, respectively, in

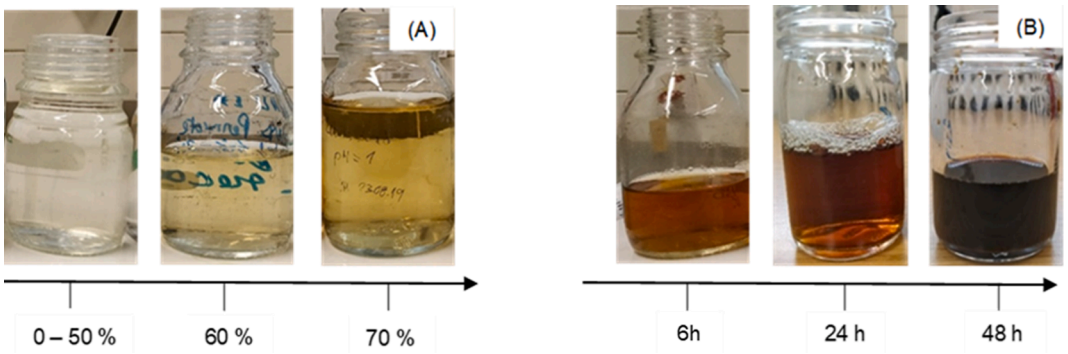

Fig. 5. Color observation of A) condensates at different recoveries and B) condensates at 80% recovery over time.

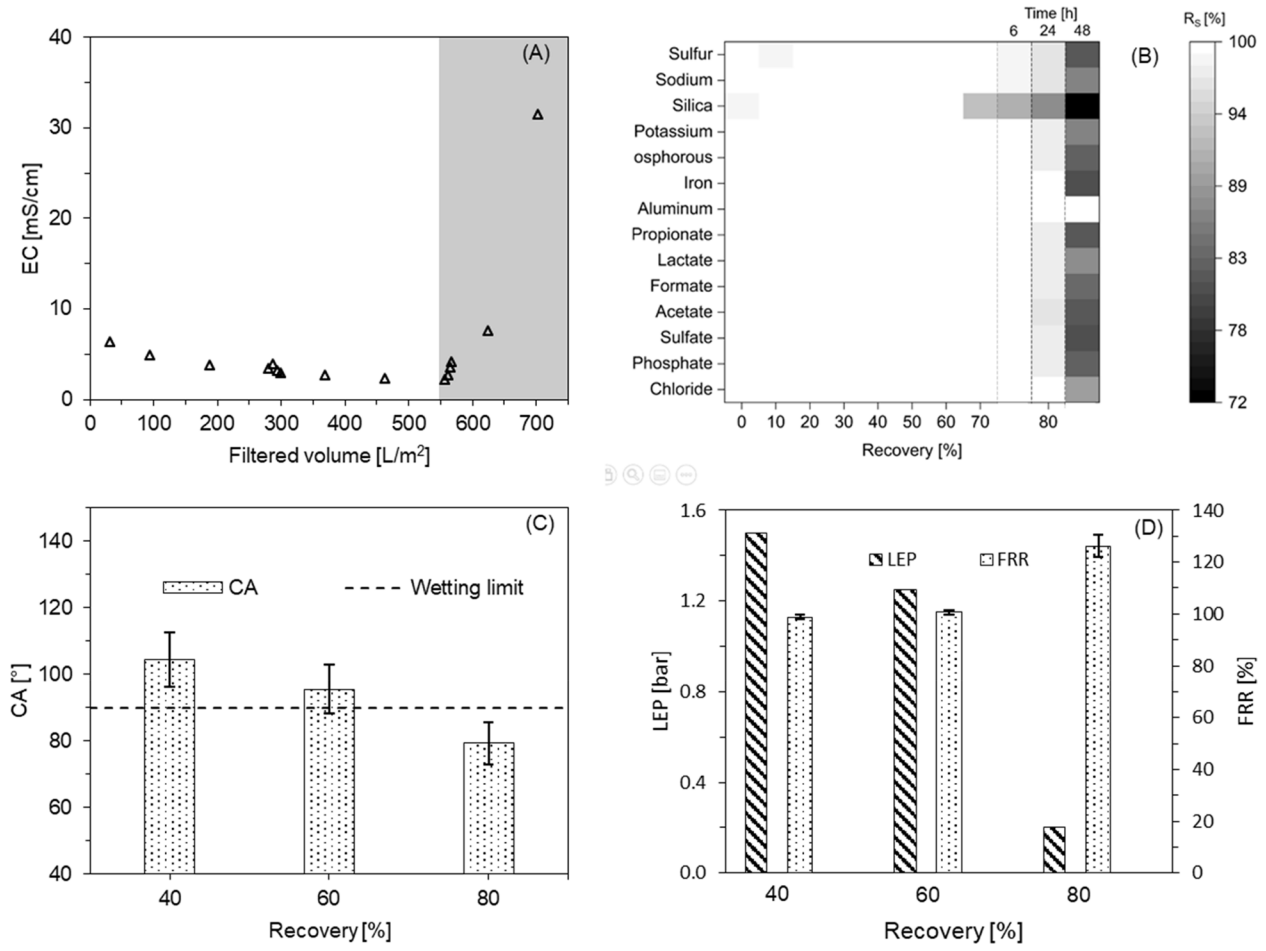

Fig. 6. A) Electrical conductivity in condensate; until 560 L/m^2 filtered volume the values are from experiment 5 and the remaining are from experiment 6 (The grey area depicts the point at which the rise in electrical conductivity was observed), B) Solute retention (R_S) at different recoveries, C) Comparison of contact angles and D) Comparison of liquid entry pressure (LEP) and flux recovery ratio (FRR) among experiments 4 to 6 based on different recoveries of 40%, 60% and 80%.

comparison with experiment 4. A liquid entry pressure of 0.2 bar (experiment 6) after 80% recovery is extremely low, and depicts the higher risk of membrane wetting.

Moreover, after cleaning with demineralized water, flux recovery ratios (FRR) for experiments 4 and 5 were around 100% ± 1%. This indicates that the simple cleaning via demineralized water was enough to recover the pure water flux. Hence, the fouling until 60% recovery was reversible even without the need for any cleaning procedures. In contrary, for experiment 6, FRR ratio increased to 126% ± 4%. This significant increase, corroborates the loss of the membrane's hydrophobicity.

3.5. *Wetting mechanisms*

Wetting can be either instantaneous or progressive.[37] Instantaneous wetting happens when transmembrane pressure (ΔP) exceeds the liquid entry pressure (LEP). However, a transitional phase was visualized during concentrating of the feed. Hence, it was concluded that the wetting observed was rather progressive. This meant that the cross-flow velocity (CFV) used in this study did not induce a pressure that was higher than the LEP.

Progressive wetting is a result of presence of surfactants, which can readily adsorb onto a hydrophobic surface immersed in water and are very effective in reducing liquid surface tension, leading to the reduction of the LEP to be below the ΔP value even with very low concentration of surfactants.[37] Surfactants have a hydrophobic tail and a hydrophilic head, and its adsorption happens mainly due to the hydrophobic interaction between the tail and the membrane surface.

Until the recovery of 60%, no significant concentrations of surfactants could be found in the condensate. This reveals that they are remaining in the feed solution, or are adsorbed on the hydrophobic membrane surface. Supposing that no adsorption happens, it would have been expected that the normalized feed concentration increases to 167% at 40% recovery and 250% at 60% recovery. Yet the values were much lower. For instance, with 40% recovery at the end of experiment 4, the normalized feed concentration of anionic surfactants increases only up to 133%, while that of cationic and non-ionic surfactants remain around 100% (Fig. 7). This reveals that at this recovery, around half of the increased concentration of anionic surfactants were adsorbed on the membrane surface, while in the case of cationic and non-ionic surfactants, the same happened for almost all the increased concentrations. This proves that surfactants adsorbed heavily on the membrane surface. The increase of non-ionic and cationic surfactants concentrations in the feed solution throughout the different recoveries were more restrained in comparison to that of anionic surfactants. This implies that adsorptions of non-ionic and cationic surfactants on the membrane surface are higher than that of anionic surfactants. The reason might be the electrostatic repulsion between anionic surfactants and the negatively charged ePTFE membrane (at pH value of 9). On the other hand, the latter forms an electrostatic interaction with the positively charged heads of the cationic surfactants, possibly leading to an increased adsorption on the membrane surface. Furthermore, the hydrophilic-lipophilic balance (HLB) highly influences the adsorption of surfactants, wherein low HLB implies higher hydrophobicity and thus higher

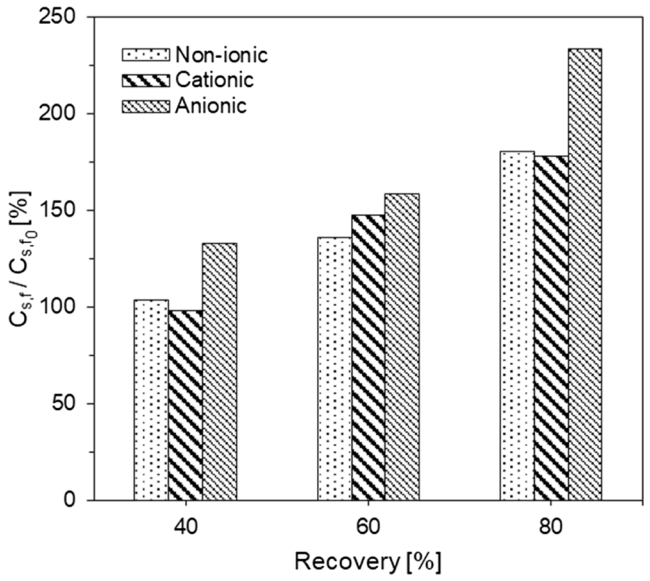

Fig. 7. Normalized feed concentration $\left(C_f/C_{f_0}\right)$ of surfactants among experiments 4 to 6 based on different recoveries of 40%, 60% and 80%.

adsorption.[38] As the surfactant tail adsorbs on the membrane surface, surfactants move from the bulk solution to the pores of the membrane. Meanwhile water is dragged by the hydrophilic head into the pores, filling it and hence stimulating wetting.[17] In general, non-ionic surfactants have lower HLB values than ionic surfactants. As a result, it is always expected that non-ionic surfactants would adsorb faster on the membrane surface.

4. Conclusions

This study demonstrates the impact of MD in treating HTL-WW_{UF}. In air gap membrane distillation, the membrane proved its rigidity under a wide range of feed temperatures from 30 °C up to 60 °C as well as at long term operations up to 36 days. Among different feed temperatures, 60 °C was found to be optimal due to the highest recovery of ammonium in the condensate and the highest flux. However, an adverse effect through TOC contamination was observed, hence feed temperatures above 60 °C would not be recommended. Condensate recovery until approximately 80% was trialed using several analytical methods, 60% was found to be the ideal one, above which membrane wetting was unavoidable. The effect of surfactant adsorption, mainly non-ionic and cationic surfactants, on the membrane surface was highly influential in accelerating the onset of wetting.

CRediT authorship contribution statement

Ali Sayegh: Conceptualization, Methodology, Investigation, Data curation, Writing – original draft. **Nikhil Shylaja Prakash:** Investigation, Data curation. **Harald Horn:** Writing – review & editing, Supervision, Funding acquisition. **Florencia Saravia:** Conceptualization, Validation, Writing – review & editing, Supervision, Funding acquisition.

Declaration of Competing Interest

The authors declare that they have no known competing financial interests or personal relationships that could have appeared to influence the work reported in this paper.

Acknowledgements

This project has received funding from the European Union's Horizon 2020 Research and Innovation Programme under Grant Agreement No. 818413. (NextGenRoadFuel - Sustainable Drop-In Transport fuels from Hydrothermal Liquefaction of Low Value Urban Feedstocks)

The authors would like to thank Steeper Energy (https://steeper-energy.com/) for the processing of the sludge and supply of the water phase used for the study.

The authors would like to thank the KIT Research Laboratories at the Engler-Bunte-Institut Water Chemistry and Water Technology, and the DVGW research center at the Engler-Bunte-Institut.

Axel Heidt, Ulrich Reichert, Reinhard Sembritzki and Matthias Weber (Engler-Bunte-Institut) are acknowledged for their assistance in laboratory experiments.

Appendix A. Supplementary material

Supplementary data to this article can be found online at https://doi.org/10.1016/j.seppur.2021.120379.

References

[1] R. Castro-Amoedo, T. Damartzis, J. Granacher, F. Maréchal, System Design and Performance Evaluation of Wastewater Treatment Plants Coupled With Hydrothermal Liquefaction and Gasification, Front. *Energy Res* 8 (2020), 568465.
[2] X.i. Zhang, X. Li, R. Li, Y. Wu, Hydrothermal Carbonization and Liquefaction of Sludge for Harmless and Resource Purposes: A Review, Energy Fuels 34 (11) (2020) 13268–13290.
[3] S.S.A. Syed-Hassan, Y.i. Wang, S. Hu, S. Su, J. Xiang, Thermochemical processing of sewage sludge to energy and fuel: Fundamentals, challenges and considerations, Renew. Sustain. Energy Rev. 80 (2017) 888–913.
[4] T.E. Seiple, R.L. Skaggs, L. Fillmore, A.M. Coleman, Municipal wastewater sludge as a renewable, cost-effective feedstock for transportation biofuels using hydrothermal liquefaction, J. Environ. Manage. 270 (2020) 110852, https://doi.org/10.1016/j.jenvman.2020.110852.
[5] M. Pham, L. Schideman, J. Scott, N. Rajagopalan, M.J. Plewa, Chemical and biological characterization of wastewater generated from hydrothermal liquefaction of Spirulina, Environ. Sci. Technol. 47 (4) (2013) 2131–2138.
[6] Y. Zhou, L. Schideman, M. Zheng, A. Martin-Ryals, P. Li, G. Tommaso, Y. Zhang, Anaerobic digestion of post-hydrothermal liquefaction wastewater for improved energy efficiency of hydrothermal bioenergy processes, Water Sci. Technol. 72 (12) (2015) 2139–2147.
[7] D.C. Elliott, P. Biller, A.B. Ross, A.J. Schmidt, S.B. Jones, Hydrothermal liquefaction of biomass: developments from batch to continuous process, Bioresour. Technol. 178 (2015) 147–156.
[8] M. Minarick, Y. Zhang, L. Schideman, Z. Wang, G. Yu, T. Funk, D. Barker, Product and economic analysis of direct liquefaction of swine manure, Bioenergy Res. 4 (4) (2011) 324–333.
[9] M. Zheng, L.C. Schideman, G. Tommaso, W.-T. Chen, Y. Zhou, K. Nair, W. Qian, Y. Zhang, K. Wang, Anaerobic digestion of wastewater generated from the hydrothermal liquefaction of Spirulina: Toxicity assessment and minimization, Energy Convers. Manage. 141 (2017) 420–428.
[10] S. Ruixia, et al., Effects of organic strength on performance of microbial electrolysis cell fed with hydrothermal liquefied wastewater, Int. J. Agric. Biol. Eng. 10 (2017) 206–217.
[11] H. Lyu, Y. Fang, S. Ren, K. Chen, G. Luo, S. Zhang, J. Chen, Monophenols separation from monosaccharides and acids by two-stage nanofiltration and reverse osmosis in hydrothermal liquefaction hydrolysates, J. Membr. Sci. 504 (2016) 141–152.
[12] X. Zhang, J. Scott, B.K. Sharma, N. Rajagopalan, Advanced treatment of hydrothermal liquefaction wastewater with nanofiltration to recover carboxylic acids, Environ. Sci. Water Res. Technol. 4 (4) (2018) 520–528.
[13] B. Díez, R. Rosal, A critical review of membrane modification techniques for fouling and biofouling control in pressure-driven membrane processes, Nanotechnol. Environ. Eng. 5 (2020) 1–21.
[14] A. Alkhudhiri, N. Darwish, N. Hilal, Membrane distillation: A comprehensive review, Desalination 287 (2012) 2–18.
[15] S. Goh, J. Zhang, Y.u. Liu, A.G. Fane, Fouling and wetting in membrane distillation (MD) and MD-bioreactor (MDBR) for wastewater reclamation, Desalination 323 (2013) 39–47.
[16] A.C.M. Franken, J.A.M. Nolten, M.H.V. Mulder, D. Bargeman, C.A. Smolders, Wetting criteria for the applicability of membrane distillation, J. Membr. Sci. 33 (3) (1987) 315–328.
[17] N.G.P. Chew, S. Zhao, C.H. Loh, N. Permogorov, R. Wang, Surfactant effects on water recovery from produced water via direct-contact membrane distillation, J. Membr. Sci. 528 (2017) 126–134.
[18] F. Kamranvand, C.J. Davey, L. Williams, A. Parker, Y. Jiang, S. Tyrrel, E. J. McAdam, Ultrafiltration pretreatment enhances membrane distillation flux,

resilience and permeate quality during water recovery from concentrated blackwater (urine/faeces), Sep. Purif. Technol. 253 (2020) 117547, https://doi.org/10.1016/j.seppur.2020.117547.
[19] M.B. Vanotti, A.A. Szogi, Use of gas-permeable membranes for the removal and recovery of ammonia from high strength livestock wastewater, Proc. Water. environ. Fed. 2011 (1) (2011) 659–667.
[20] M.C. Garcia-González, M.B. Vanotti, Recovery of ammonia from swine manure using gas-permeable membranes: Effect of waste strength and pH, Waste Manage. 38 (2015) 455–461.
[21] B. Riaño, B. Molinuevo-Salces, M.B. Vanotti, M.C. García-González, Application of gas-permeable membranes for-semi-continuous ammonia recovery from swine manure, Environments 6 (3) (2019) 32, https://doi.org/10.3390/environments6030032.
[22] A. Sayegh, N. Shylaja Prakash, T.H. Pedersen, H. Horn, F. Saravia, Treatment of hydrothermal liquefaction wastewater with ultrafiltration and air stripping for oil and particle removal and ammonia recovery, J. Water Process Eng. 44 (2021) 102427, https://doi.org/10.1016/j.jwpe.2021.102427.
[23] A. Bauer, M. Wagner, F. Saravia, S. Bartl, V. Hilgenfeldt, H. Horn, In-situ monitoring and quantification of fouling development in membrane distillation by means of optical coherence tomography, J. Membr. Sci. 577 (2019) 145–152.
[24] G. Veréb, et al., Intensification of the ultrafiltration of real oil-contaminated (produced) water with pre-ozonation and/or with TiO 2, TiO 2/CNT nanomaterial-coated membrane surfaces, Environ. Sci. Pollut. Res. 27 (2020) 1–11.
[25] T.Y. Cath, V.D. Adams, A.E. Childress, Experimental study of desalination using direct contact membrane distillation: a new approach to flux enhancement, J. Membr. Sci. 228 (1) (2004) 5–16.
[26] J. Li, Y. Guan, F. Cheng, Y.u. Liu, Treatment of high salinity brines by direct contact membrane distillation: Effect of membrane characteristics and salinity, Chemosphere 140 (2015) 143–149.
[27] L. Martínez, Comparison of membrane distillation performance using different feeds, Desalination 168 (2004) 359–365.
[28] M.S. EL-Bourawi, M. Khayet, R. Ma, Z. Ding, Z. Li, X. Zhang, Application of vacuum membrane distillation for ammonia removal, J. Membr. Sci. 301 (1-2) (2007) 200–209.
[29] Huang, J.-C. & Shang, C. in *Advanced physicochemical treatment processes* 47-79 (Springer, 2006).
[30] Z. Xie, T. Duong, M. Hoang, C. Nguyen, B. Bolto, Ammonia removal by sweep gas membrane distillation, Water Res. 43 (6) (2009) 1693–1699.
[31] M.C. Carnevale, E. Gnisci, J. Hilal, A. Criscuoli, Direct contact and vacuum membrane distillation application for the olive mill wastewater treatment, Sep. Purif. Technol. 169 (2016) 121–127.
[32] P.J.L. Derikx, H.C. Willers, P.J.W. ten Have, Effect of pH on the behaviour of volatile compounds in organic manures during dry-matter determination, Bioresour. Technol. 49 (1) (1994) 41–45.
[33] F. Ricceri, M. Giagnorio, G. Farinelli, G. Blandini, M. Minella, D. Vione, A. Tiraferri, Desalination of produced Water by Membrane Distillation: Effect of the feed components and of a pre-treatment by fenton oxidation, Sci. Rep. 9 (1) (2019), https://doi.org/10.1038/s41598-019-51167-z.
[34] K.W. Lawson, D.R. Lloyd, Membrane distillation, J. Membr. Sci. 124 (1) (1997) 1–25.
[35] D.K. Patil, S.P. Shirsat, Membrane distillation review and flux prediction in direct contact membrane distillation process, Int Res J Eng Technol (IRJET) 4 (2017) 829–845.
[36] P. Biniaz, N. Torabi Ardekani, M. Makarem, M. Rahimpour, Water and wastewater treatment systems by novel integrated membrane distillation (MD), ChemEngineering 3 (1) (2019) 8, https://doi.org/10.3390/chemengineering3010008.
[37] T. Horseman, Y. Yin, K.SS. Christie, Z. Wang, T. Tong, S. Lin, Wetting, scaling, and fouling in membrane distillation: State-of-the-art insights on fundamental mechanisms and mitigation strategies, ACS ES&T Eng. 1 (1) (2021) 117–140.
[38] P.-J. Lin, M.-C. Yang, Y.-L. Li, J.-H. Chen, Prevention of surfactant wetting with agarose hydrogel layer for direct contact membrane distillation used in dyeing wastewater treatment, J. Membr. Sci. 475 (2015) 511–520.